

# Measuring Cell Forces by a Photoelastic Method

Adam Curtis, Lucia Sokolikova-Csaderova, and Gregor Aitchison

Centre for Cell Engineering, University of Glasgow, Glasgow G12 8QQ, United Kingdom

**ABSTRACT** A new method for measuring the mechanical forces exerted by cells on the substratum and through the substratum to act on other cells is described. This method depends upon the growth of cells on a photoelastic substratum, polydimethylsiloxane coated with a near monolayer of fibronectin. Changes in the forces applied by the cells to the substratum lead to changes in birefringence, which can be measured and recorded by the Polscope computer-controlled polarizing microscope. The changes in azimuth and retardance can be measured. A method for calibrating the stress is described. The method is sensitive down to forces of 1 pN per square microns. Fairly rapid changes with time can be recorded with a time resolution of  $\sim 1$  s. The observations show that both isolated adhering, spread cells and also cells close to contact exert stresses on the substratum and that the stresses are those that would be produced by forces of 10–1000 pN per cell. The forces are almost certainly exerted on nearby cells since movement of one cell causes strains to appear around other nearby cells. The method has the defect that strains under the cells, though detectable in principle, are unclear due to birefringence of the components of the cytoplasm and nucleus. It is of special interest that the strains on the substratum can change in the time course of a few seconds and appear to be concentrated near the base of the lamellipodium of the cell as though they originated there. As well as exerting forces on the substratum in the direction of the long axis of the cell, appreciable forces are exerted from the lateral sides of the cell. The observations and measurements tend to argue that microtopography and embedded beads can concentrate the forces.

## INTRODUCTION

Mechanical forces acting on cells affect many processes such as proliferation, cytoskeletal expression (1), and gene activity (2). Often these forces may be applied from external sources, e.g., muscular activity in remote parts of the body. But in addition the cells can act on their near neighbors (3).

Recently a number of novel methods for measuring the forces generated by individual cells have been reported (4–7). These methods, though highly ingenious and useful, measure the forces required either to deform microstructures on the substratum beneath the cell (5,6) or displace marker beads embedded in the substratum close to the cell (7). The possibility exists, as has been allowed by Bershadsky et al. (4), that the heterogeneous mechanical nature of the substratum (pillars or embedded particles) modifies the forces the cell can exert, almost as exercise machines in the gymnasium influence the athlete to develop greater forces. The aim of those measurements has been directed mostly at the questions relevant to cell movement.

But forces between cells are well known to be important in events such as wound healing, especially in contracture and the pulling open of wounds, in development, and perhaps in remodeling of tissues (3).

We describe a new method, based on photoelastic measurements, particularly directed at observing the effects of pairs of cells on each other or on small groups and also providing a method unimpaired by the presence of a heterogeneous substrate. Thus we test whether such substrates with micrometric topographic details modify cell force generation or application. The method has already been used

(8) to detect active transverse contractions in fibroblasts in addition to the well-known longitudinal contractions in such cells. It can also detect forces acting between cells when there is microscopically visible separation between them. A further possible advantage of this technique is that observations can be made at fairly short-term and repetitive intervals over long periods, thus revealing whether rapid changes or fluctuations occur.

Measurement of the forces exerted by cells on their surroundings has been achieved by a variety of methods. Basically nearly all these methods set up situations where the cells distort their surroundings in a detectable way and where the situation is sufficiently simple and reproducible to allow calibration of the distortion that a given force applies. Harris (9) introduced the idea of growing cells in a thin membrane and observing the distortion. Those early results were not calibrated but indicated that fibroblasts develop forces sufficient to distort a thin elastic membrane.

Thus it would be appropriate to introduce a method where the substratum is effectively isotropic at least at the start of the experiment. We have grown cells on an isotropic substratum and looked for distortion of that substratum by forces exerted on it by the cells. The method we describe relies on the detection of such distortion by photoelasticity; see Huard (10) for a description of the principles of photoelasticity or Zhao et al. (11) for details of the method applied to strain distribution in a composite material.

## MATERIALS AND METHODS

Cells: h-tert fibroblasts (human) (Clontech, UK), B10 D2 (otherwise known as LeII) mouse capillary endothelia (from laboratory stocks), and HGTFN (human granuloma endothelia also derived from laboratory stocks) were

*Submitted May 15, 2006, and accepted for publication November 27, 2006.*

Address reprint requests to Adam Curtis, E-mail: a.curtis@bio.gla.ac.uk.

© 2007 by the Biophysical Society

0006-3495/07/03/2255/07 \$2.00

doi: 10.1529/biophysj.106.088849

grown on the polydimethylsiloxane surfaces which had been coated with appropriate adhesion proteins such as fibronectin for various periods (1–4 days) and the cultures then examined at 37° C with the Polscope microscope.

The Polscope Microscope (CRI International, Woburn, MA) was mainly used with 40× and 100× strain-free objectives. The microscope with its associated software can measure retardances down to 0.1 nm (manufacturer's handbook) and azimuths as well. Pseudocolor images can be obtained which are useful for rapid survey observations and for revealing any mis-set up of the optical system; but for serious observation, images stamped with retardances at various points on the image are most useful. Images of birefringence were obtained after a number of images of the bare poly (dimethyl siloxane) (PDMS) surfaces and a number of phase contrast images of the cells at areas where the birefringence was to be measured. The images of the bare PDMS surface were obtained to check that there was no strain in the substratum in the absence of cells. This check validates the points on the origin in the graph in Fig. 1. The phase contrast images of the sampling areas were acquired so that the exact boundaries of the cell or cells could be established. Three images of each area to be measured were taken in quick succession, one for acquiring the raw birefringence data and two for further processing (for pseudocoloring, obtaining retardance transects across parts of the field, and stamping of calculated retardance values). This method can also be used for measuring forces over a time series. Time-lapse video image sets were acquired over short periods (30–90 min) to record possible rapid changes in forces.

On many of the images in this work code numbers appear in the bottom right-hand corner: these are the original image filing names from the Polscope. Parts of the date and time may also appear just to the left of the file name.

The images obtained with the Polscope, running in the retardance mode, of isotropic materials were effectively black with a noise level of <0.2%. Each set of measurements made started with a test of isotropic PDMS to show that the noise level met this criterion. When examining cultures of cells on PDMS with the display in the retardance mode, any areas whiter than the noise level indicate birefringence with the whitest parts of the display corresponding to appreciable retardances.

## Calibration

The calibration of the Polscope measurements was based on the measured retardance which developed in PDMS films as a response to a known applied

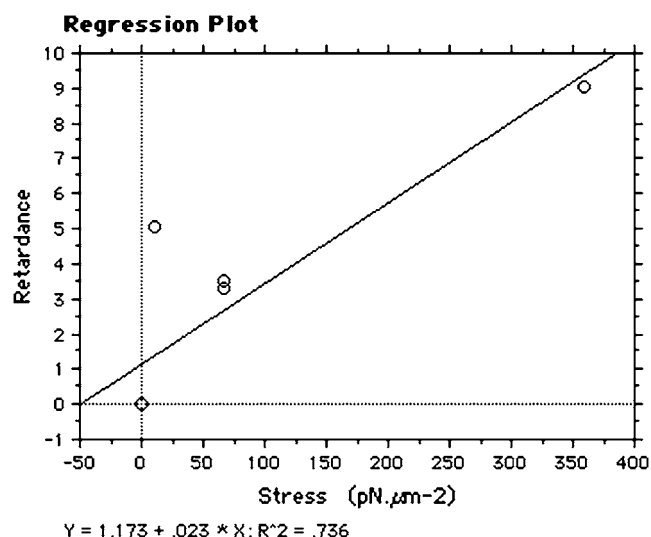


FIGURE 1 Calibration of stress against retardance. Note that retardances measured (see later) mostly are in the piconewton range. Retardance in nanometers. Stress in units of  $10^{-12}$  N/ $\mu$ m.

force and its comparison with modeling of the same structure and its loading. Finite element modeling allows determination of the strain and stress distribution due to a given set of loading and boundary conditions applied to a structure whose material properties are known.

The PDMS structure for Polscope measurements was prepared as follows: PDMS uncured was made by mixing 10 parts of SYLGARD 184 and 1 part of curing agent (both supplied as type 184 by Dow Corning, Wiesbaden, Germany) and sandwiching a thin film between two polystyrene coverslips or alternatively (and better) polystyrene flexible sheets. These "sandwiches" were then placed in a heated oven at 90° C for 16 h and the coverslips or covering sheets removed to acquire sheets of cured PDMS. The sheets were allowed to overhang a glass coverslip by a known distance. The force was thus applied by the weight of a free edge of Sylgard. Retardance values were measured along transects crossing the edge of the film and the edge of its support at or close to the central axis of the film.

The structure described above was modeled with finite element analysis, using an elasticity modulus of 2.02 MPa and a Poisson ratio of 0.49 (5). Elasticity moduli were measured according to Pelham and Wang (12) by suspending known masses at the end of PDMS strips. Elasticity moduli were measured according to Pelham and Wang (12) by suspending known masses at the end of PDMS strips. Finite element analysis (Abaqus program, Hibbit, Karlsson & Sorensen, Providence, RI, available under academic license) was used in the process of calibration. First, the PDMS sheet was loaded with a known force and resulting retardance values were measured experimentally. Then, the whole situation was modeled by finite element analysis with corresponding loading and boundary conditions, and the PDMS was modeled as a mesh of nodes having appropriate elastic properties. The stress values caused by the applied force were calculated in each node, and then these are linked to the measured retardance values as there is a relation between stresses and retardance for birefringence imaging.

The loading caused by gravity acting on overhanging PDMS sheets results in an axial stress field. Stress values in nodes of the top plane of the model mesh were used for comparison with the measured retardance based on the following relationship:  $R = C \times d \times \Delta s$ , where  $C$  is the optical stress coefficient being the material constant,  $d$  is the thickness of the PDMS film, and  $\Delta s$  is the difference between values of principal stresses. In this case, principal stresses are in-plane stresses in  $x$  and  $y$  directions and, the  $z$  stress component is at least by one order of magnitude smaller and is neglected. As changes in thickness are small (<0.01% according to the model),  $d$  is considered constant, and a relationship between retardance values measured at a certain position of the film and values of calculated principal stresses difference at this position should exist. The area at the border of a free-hanging part of the film and the fixed part was used for this purpose as the strain should reach maximum values at that position. Only the data from the smallest overhangs were used since it is under these conditions that strains will be nearest to uniaxial.

Based on our modeling, measured retardance values of units of nanometers of retardance correspond to the stress range of  $10^{-12}$  to  $10^{-11}$  N/ $\mu$ m<sup>2</sup>. It is necessary to bear in mind that in case of cells exerting biaxial stress at a certain point, the resulting measured retardance will correspond to the difference of these two stress components and hence the stress caused by the cell can appear smaller. An alternative and less rigorous method of relating retardances to stresses is to use the Coulomb approach (13), which results in similar values. The azimuths of the strongest retardances were also recorded, which allows the experimenter to observe the directions of strongest force development.

## RESULTS

### Cell death

The first requirement is to show that the strain seen in the substrate disappears when the cell is dead. To test this, images are collected of a cell before killing and afterwards.

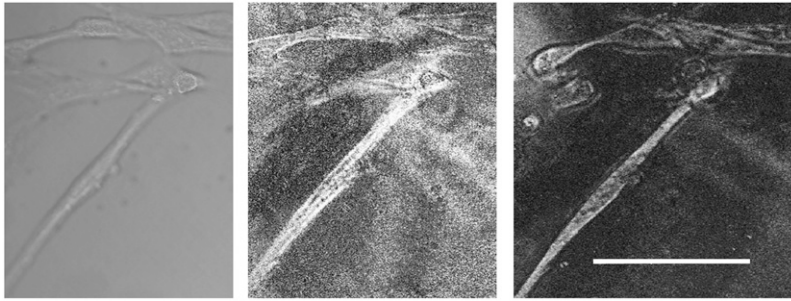


FIGURE 2 Different types of image and of dying cells left-hand (LH) view. Several h-tert fibroblasts seen under phase contrast illumination, center view. The same cells seen under retardance imaging showing much retardance variation between the cells indicating development of strain. Right-hand (RH) figure. The same cells 5 min after fixation with SDS. Nearly all strain between the vanished. Note that in this and other images of cells the regions between cells showing degrees of gray tone indicative of an appreciable retardance. Uncompensated images show virtually transparent regions between cells. 40 $\times$  objective; scale bar, 50  $\mu$ m.

The cells were killed by infusion of a 0.1% v/v solution of sodium dodecyl sulfonate (SDS) (Sigma, Poole, UK) in phosphate-buffered saline, pH 7.6, ionic strength 0.15 (see Fig. 2).

### Cells on a rigid isotropic substratum

The second calibration test is to grow the cells on a rigid glass substratum which will not show photoelastic effects. A typical result is shown in Fig. 3. This allows assessment of the contribution to the image from internal cell components which are birefringent. Cells grown on PDMS-free glass coverslips were examined in a Polscope. The images obtained (see Fig. 3) birefringent structures inside the cell but no photoelastic features outside the cells. Comparison of these images with those obtained on photoelastic substrates allows recognition of the photoelastic effects outside the cell as such. Such a comparison also suggests that parts of the images apparently inside the cells may be photoelastic effects generated in the PDMS substratum under the cell, but the images contain so much birefringence arising from within the cell that these parts of these images cannot be separated into substratum and internal cell components. These images effectively show the cytoskeleton and the edge of the cell as a thin line of birefringence with no evidence of pericellular areas of strain.

### Cells grown on a photoelastic substratum

#### *Isolated cells*

Both h-tert fibroblasts and mouse B10.D2 endothelia grown on PDMS show photoelastic effects in the substrate in the region around the cells. Typically this only extends laterally from the cells for a few tens of micrometers. It is not exhibited, or is more weakly exhibited, on the concave edges of a cell. The strongest photoelastic effect was usually observed in the region in front of a lamellopodium (see Fig. 4), but if the cell has a “necked-in” region just behind the lamellopodium this may be the region of most intense photoelastic effects just outside the cell. Azimuth plots are shown in Fig. 5. Rounded-up cells that are circular or nearly so in plan view again exhibited little or no birefringence. When cultures were cooled to room temperature, the birefringence in the substratum slowly vanished.

### Forces between neighboring but not contiguous cells

#### *Forces between cells*

The following five images (Figs. 6–10) show both contiguous groups of cells and cell and cell groups separated from each other. Note that retardances can be quite high between cells, seen as lighter zones, implying that forces in the substratum may be appreciable.

### Time-lapse video studies

Time-lapse videos were taken with the Polscope at intervals of 30–60 s. The videos, available at <http://www.gla.ac.uk/centers/cellengineering/adam/adam.html>, show surprisingly rapid changes in retardance and azimuth with strain sometimes rising or falling over periods as short as 30–120 s.

If one cell pulls on another, changes in birefringence appear to be synchronized in the two cells; but there is no evidence for more general synchronized onset (or cessation) of levels of activity, and cells close to each other may show no apparent synchronization. Despite this there seem to be

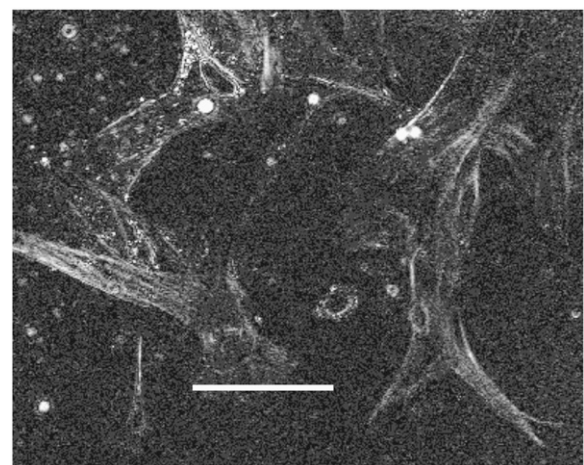


FIGURE 3 Image of h-tert human fibroblasts grown on a rigid substratum. The cell cytoskeleton is seen as well as birefringent particles in the system, perhaps a phosphate precipitated from the culture medium but no birefringence in the glass coverslip substratum. Scale bar, 40  $\mu$ m. 40 $\times$  objective retardance display.

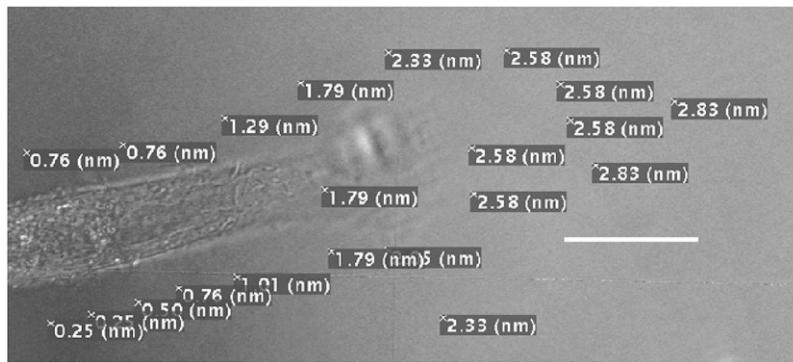


FIGURE 4 h-Tert fibroblast imaged under 100 $\times$  objective Polscope. Retardance stamped mode. Retardances in nanometers measured at point in upper LH corner of each stamp. Note relatively large retardances corresponding to stresses of  $\sim 6 \times 10^{-12} \text{ N}/\mu\text{m}^2$  extending far over the substratum (PDMS) in front of the cell and the smaller forces along the sides of the cell. Scale bar, 15  $\mu\text{m}$ .

zones of activity, and these may correspond to changes in cell shape preceding and after cell division.

## SUMMARY

1. Stresses of  $\sim 1\text{--}50 \text{ pN}/\mu\text{m}^2$  are generated around fibroblasts and other cells. Such values are lower than those reported by some other authors.
2. These are often strong on the lateral sides of the lamellipodium as well as in front of it and appear to be associated with transverse contractions in the cell.
3. They are also prominent laterally between fibroblasts along their contact zone.
4. Force generation is removed in 2 min by poisoning the cell's contractile mechanisms and more slowly by cooling the cells.
5. In groups of live cells in cell culture, rapid force changes and readjustments usually take place. In any group of 7–10 fibroblasts which are not close packed, there will usually be one or more cells that are not exerting mechanical stresses to strain themselves (see video time-lapse sequences).

The strain that the cells cause in the PDMS surface is too small to be easily observable as a dimensional change; but 1 millistrain means that for a typical cell only 20-  $\mu\text{m}$  long, the dimensional change is only 20 nm. Cells are sensitive down to at least 50 microstrains (14). A relatively easily measured dimensional change of 2  $\mu\text{m}$  would correspond to 100,000 microstrains.

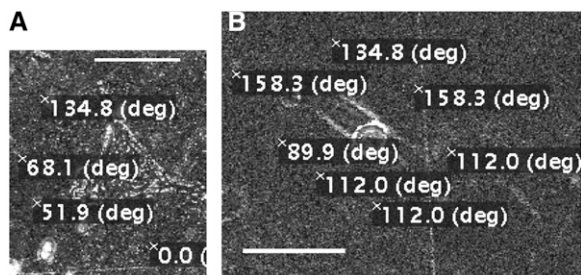


FIGURE 5 (a and b) Azimuth plots of forces around cells.

## DISCUSSION AND CONCLUSIONS

The strains in the PDMS substrate due to the activities of cells revealed by polarization microscopy are of course probably rarely uniaxial. Contraction in one axis is likely to lead to relaxation (extension) at 90° to that direction. This can best be seen, in the absence of comparative linear measurements, by azimuth plots (see Fig. 5).

Photoelasticity provides a suitable method for measuring the forces exerted by a cell on an appropriate substratum which should be transparent, isotropic when stress-free, and not too rigid to minimize reactions to stress. Besides, measuring the strain in terms of retardance photoelastic measurements can also indicate the azimuth of the polarization. Photoelastic measurement requires a fairly soft material whose Young's modulus lies in the range 10–10<sup>3</sup> kPa. Unfortunately it is not suitable for use of collagen whose intrinsic birefringence is so large that other signals are swamped. Though a signal from areas underneath the cell can be detected, this is usually so complicated by signals from the cytoskeleton that no useful quantitative information can be gained.

The method is ideal for studying interactions between neighboring cells not in optical contact and for measuring smaller forces than can be estimated by other methods. This method also has the advantage that no new physical structure has been introduced that the cells might react to. The methods introduced by Abercrombie et al. (3) and Tan et al. (6) fabricated micropillars on the surface of the culture material, and it is known (15) that cells react to such structures by cytoskeletal reorganization. Since the cytoskeleton is involved in force generation, reorganization could alter the disposition and perhaps the extent of force generation. In the case of the experiments by Dembo et al. (7) where particles were embedded in the substrate, these may have acted to redistribute forces since the force pattern should have changed because the particles could be moved. All this suggests that there is a sensitive feedback mechanical system in the cell. There is, of course, the interesting question of whether the cell is akin to a motor system that increases energy output in response to resistance to motion, a situation found par excellence in a stepping motor. If so, any

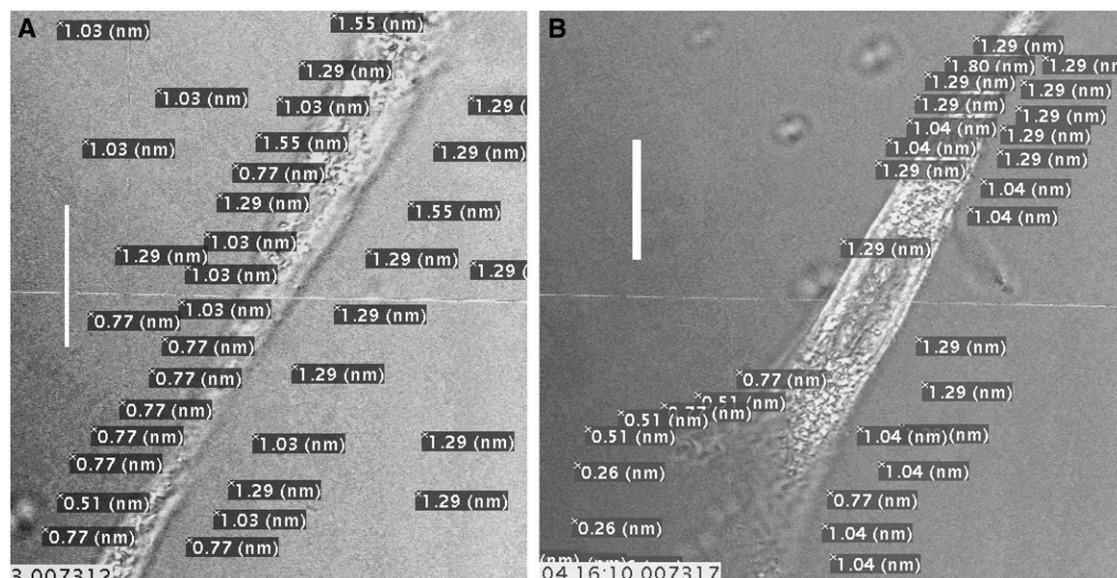


FIGURE 6 (a) Part of two h-tet fibroblasts with retardances “stamped” on image. Retardances are at points on either side of the cell showing that appreciable forces are exerted on the lateral sides of the cell. Scale bar  $20\ \mu\text{m}$ . (b) A similar cell with similar interpretation.  $100\times$  objective, scale  $15\ \mu\text{m}$ .

non-Newtonian behavior or even any constant but unusually high or low rigidity in the substrate will change the force measured. Even the photoelastic method does not escape this source of confusion, but it does allow the hypothesis to be tested.

Force mapping such as we have done does reveal that, with the exception of isolated cells, forces between groups of cells are likely to have complex and rather unpredictable distributions. We probably need to have a parallel model of the principal mechanical components in the cellular system, and this is not merely the distribution of cytoskeletal elements but also the strength with which they bind to each other.

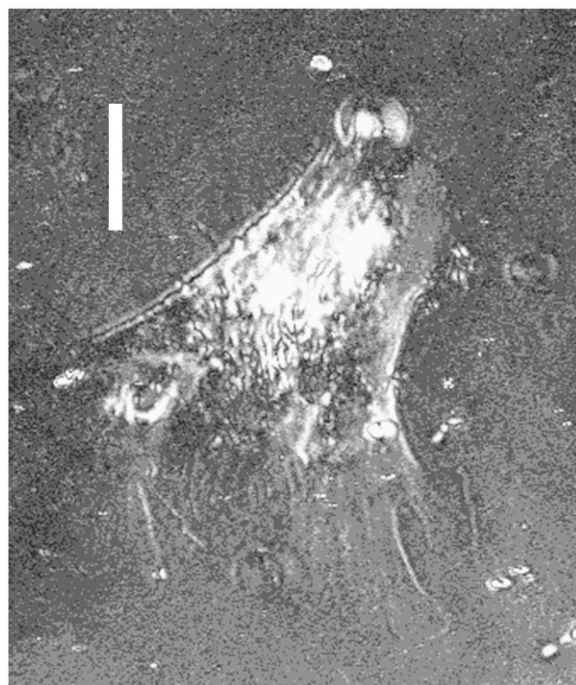


FIGURE 7 Endothelial cell (derived from human granuloma). An isolated cell seen in retardance display. Scale bar,  $15\ \mu\text{m}$ . Note darker regions at sides of the cell which are regions of low strain and the lighter regions at the front of the lamellopodium correspond to regions of greater strain.  $40\times$  objective.

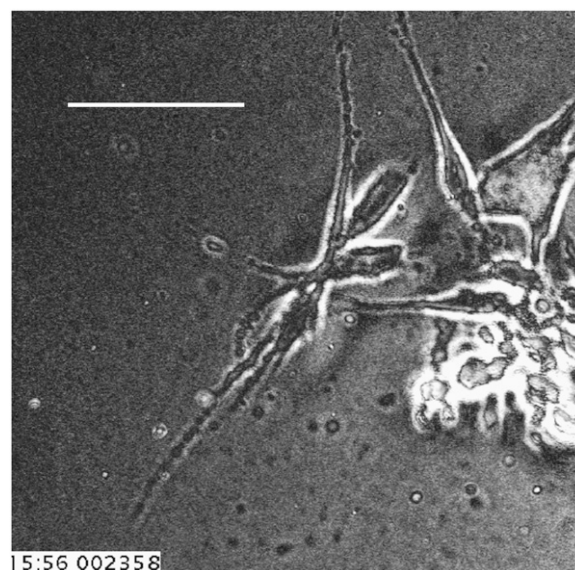


FIGURE 8 Strains in substrate between cells seen as darker and lighter zones: the lighter the zone the higher the age contrast enhanced by  $\sim 30\%$  endothelia from human granuloma (HGTFN).  $40\times$  objective; scale bar,  $60\ \mu\text{m}$ .

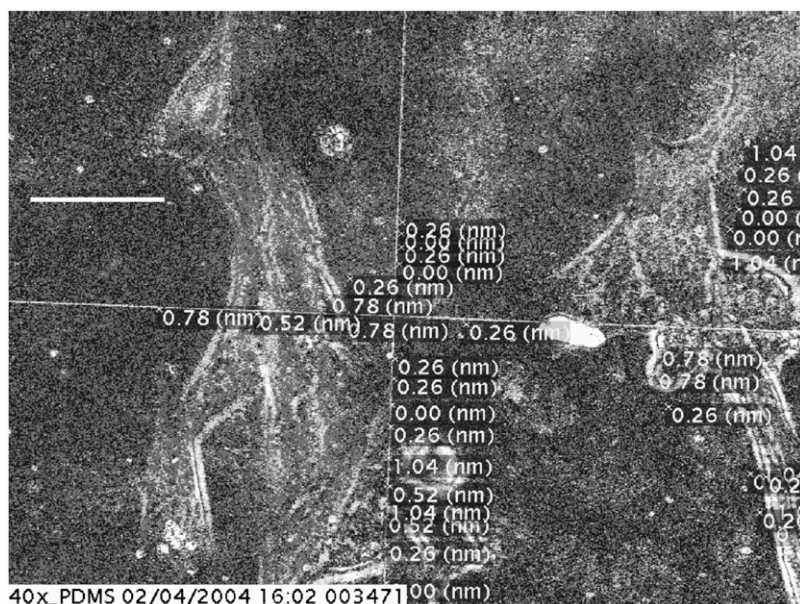


FIGURE 9 HGTFN endothelia from human granuloma. This image shows stamps of retardances at points between cells. Note that these values can be relatively high indicating strain between cells. 40 $\times$  objective. Contrast enhancement  $\sim$  30%. Scale bar, 15  $\mu$ m. Note that there are appreciable areas between cells and around cells, which are whiter than the background.

As a culture of cells proceeds by cell division toward confluence, the cell cycle dies down. We cannot observe this by polarization microscopy, but as the cell packing becomes dense though not complete, we can see some tendencies to this end at rather earlier stages in the life of the cell. This fits in well with the observations by Curtis and Seehar (16) that external mechanical stimulation stimulates the cell cycle. In a three-dimensional tissue cells might be expected to exert forces on each other when cell anchoring is not as complete as it may be on a culture plate. An interesting discussion of the likely effects on tissue building of such forces has been published (17).

The force measurements around the periphery of a cell hardly ever fall to zero, whereas some space remains between the cells, suggesting that the cells are well coupled mechanically to the substratum. If the stresses measured by this photoelasticity method are summed up around the cell periphery, the results agree generally with those reported by other methods (5–7).

The tables of cell forces in Bereiter-Hahn (18) and the values quoted by Balaban et al. (5), Tan et al. (6), and Dembo et al. (7) show a wide range of values. However, the following reasons for discrepancies between measurements by this and other methods could be present:

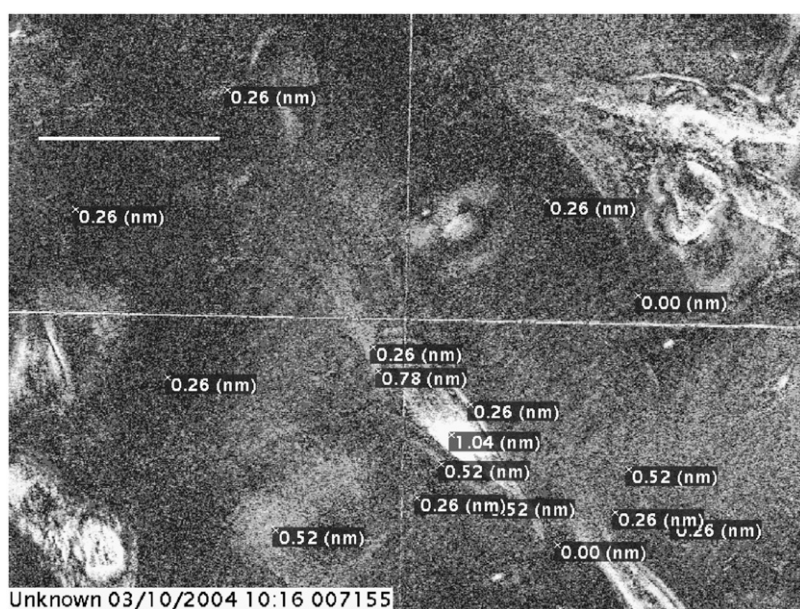


FIGURE 10 h-Tert cells. Image shows strains between cells indicated by paler gray zones or by stamps. 100 $\times$  objective. Scale bar, 40  $\mu$ m.



1. The photoelastic method does not allow measurements to be made at the extreme edge of a cell because of diffraction and resolution problems.
2. The values given in the literature correspond to forces measured in focal adhesions (underneath a cell). Our stresses are measured outside (around) the cell, as the measurement underneath a cell could be affected by birefringence from cell components. This fact is likely to contribute to smaller values of measured forces. Vectors can be obtained from the retardance and azimuth measurements.
3. The difference in substrata between the methods may affect the generation of forces by cells (see above).
4. Possibly some variation in force generation will occur between different cell types and at different stages of the cell cycle.
5. Another reason any discrepancy may arise derives from the use of micropillars (5) or embedded particles (7) in much of the work of others. Reports (19–22) on the effects of nanotopographic structures on cell adhesion, shape, and motility show that such structures have extensive effects on these properties, suggesting that force distribution and perhaps magnitude is altered by such substrata.

But it is likely that the main reason for the apparent discrepancy is the fact that the photoelastic method can be used to measure the forces just outside the perimeter of the cell which is several thousands of pixels (hundreds of microns) in extent, whereas those methods that depend on projecting pillars or embedded beads only measure forces at some scores to a few hundred sites. If the stresses are summed for the perimeter, then the forces summed for the two methods may be less discrepant.

We thank Mathis Riehle and Nicolaj Gadegaard for advice and encouragement.

The work was supported by European Commission grant BITES QLK3-CT-1999-00559 and by Scottish Higher Education Funding Council grant "Mechanotransduction Consortium". We thank these organizations.

## REFERENCES

1. Chen, C. S., and D. E. Ingber. 1999. Tensegrity and mechanoregulation: from skeleton to cytoskeleton. *Osteoarthritis Cartilage*. 7:81–94.
2. Grodzinsky, A. J., M. E. Levenston, M. Jin, and E. H. Frank. 2000. Cartilage tissue remodeling in response to mechanical forces. *Annu. Rev. Biomed. Eng.* 2:691–713.
3. Abercrombie, M., M. H. Flint, and D. W. James. 1956. Wound contraction in relation to collagen formation in scorbutic guinea pigs. *J. Embryol. Exp. Morphol.* 4:167–175.
4. Bershadsky, A. D., N. Q. Balaban, and B. Geiger. 2003. Adhesion-dependent cell mechanosensitivity. *Annu. Rev. Cell Dev. Biol.* 19:677–695.
5. Balaban, N. Q., U. S. Schwarz, D. Riveline, P. Goichberg, G. Tzur, I. Sabanay, D. Mahalu, S. Safran, A. Bershadsky, L. Addadi, and B. Geiger. 2001. Force and focal adhesion assembly: a close relationship studied using elastic micropatterned substrates. *Nat. Cell Biol.* 3:466–472.
6. Tan, J. L., J. Tien, D. M. Pirone, D. S. Gray, K. Bhadriraju, and C. S. Chen. 2003. Cells lying on a bed of microneedles: an approach to isolate mechanical force. *Proc. Natl. Acad. Sci. USA*. 100:1484–1489.
7. Dembo, M., T. Oliver, T. Ishihara, and A. K. Jacobson. 1996. Imaging the traction stresses exerted by locomoting cells with the elastic substratum method. *Biophys. J.* 70:2008–2022.
8. Curtis, A. S. G., G. Aitchison, and T. Tsapikouni. 2006. Orthogonal (transverse) arrangements of actin in endothelia and fibroblasts. *J. R. Soc. Interface*. 3:753–756.
9. Harris, A. K. 1982. Traction, and its relations to contraction in tissue cell locomotion. In *Cell Behaviour. A Tribute to Michael Abercrombie*. R. Bellairs, A. Curtis, and G. Dunn, editors. Cambridge University Press, Cambridge. 109–134.
10. Huard, S. 1997. Polarization of Light. G. Vacca, translator. John Wiley & Sons, New York.
11. Zhao, F. M., S. A. Hayes, E. A. Patterson, R. J. Young, and F. R. Jones. 2003. Measurement of micro stress fields in epoxy matrix around a fibre using phase-stepping automated photoelasticity. *Compos. Sci. Technol.* 63:1783–1787.
12. Pelham, R. J. J., and Y. Wang. 1999. High resolution detection of mechanical forces exerted by locomoting fibroblasts on the substrate. *Mol. Biol. Cell*. 10:935–945.
13. Patnaik, S. N., and S. N. Hopkins. 2004. Strength of Materials: A Unified Theory. Elsevier, Amsterdam.
14. el Haj, A. J., S. J. Minter, S. C. Rawlinson, R. Suswillo, and L. E. Lanyon. 1990. Cellular responses to mechanical loading in vitro. *J. Bone Miner. Res.* 5:923–932.
15. Curtis, A. S. G., and P. Clark. 1990. The effects of topographic and mechanical properties of materials on cell behaviour. *Crit. Rev. Biocompat.* 5:343–362.
16. Curtis, A. S. G., and G. M. Seechar. 1978. The control of cell division by tension or diffusion. *Nature*. 274:52–53.
17. Bischofs, I. B., and U. S. Schwarz. 2003. Cell organization in soft media due to active mechanosensing. *Proc. Natl. Acad. Sci. USA*. 100:9274–9279.
18. Bereiter-Hahn, J. 1987. Mechanical principles of architecture of eukaryotic cells. In *Cytomechanics*. J. Bereiter-Hahn, O. R. Anderson, and W.-E. Reif, editors. Springer-Verlag, Berlin. 3–33.
19. Curtis, A. S. G., B. Casey, J. D. Gallagher, D. Pasqui, M. A. Wood, and C. D. W. Wilkinson. 2001. Substratum nanotopography and the adhesion of biological cells. Are symmetry or regularity of nanotopography important? *Biophys. Chem.* 94:275–283.
20. Curtis, A. S. G., N. Gadegaard, M. J. Dalby, M. O. Riehle, C. D. W. Wilkinson, and G. Aitchison. 2004. Cells react to nanoscale order and symmetry in their surroundings. *IEEE Trans. Nanobioscience*. 3:61–65.
21. Dalby, M. J., M. O. Riehle, H. J. Johnstone, S. Affrossman, and A. S. Curtis. 2003. Nonadhesive nanotopography: fibroblast response to poly(*n*-butyl methacrylate)-poly(styrene) demixed surface features. *J. Biomed. Mater. Res. A*. 67:1025–1032.
22. Dalby, M. J., D. Giannaras, M. O. Riehle, N. Gadegaard, S. Affrossman, and A. S. G. Curtis. 2004. Rapid fibroblast adhesion to 27 nm high polymer demixed nano-topography. *Biomaterials*. 25:77–83.